Desalination and Water Treatment
www.deswater.com
doi: 10.5004/dwt.2021.26783

219 (2021) 113–121
April

Using GIS and RUSLE to study on the geographical distribution characteristics of soil erosion on the Dianchi Watershed, China

Shuangyun Peng

Faculty of Geography, Yunnan Normal University, Kunming 650000, China, email: 258436452@qq.com

Received 15 August 2020; Accepted 23 November 2020

ABSTRACT

Soil erosion is the primary cause of land degradation, which directly leads to ecological environment deterioration. Nowadays, soil erosion has grown up to be a global public nuisance and have menaced the surviving of human being and the development of society. Fully understanding the soil erosion distribution characteristics is of great significance for formulating reasonable and effective control measures. Based on the RUSLE model and GIS technology, this paper quantitatively analyses soil erosion distribution characteristics in Dianchi watershed, explores the relationship between erosion and topography, such as elevation and slope. The results show that the erosion amount of Dianchi watershed in 2014 was 2,250,100 t a^{-1}, and the average erosion modulus was 861.09 t km^{-2} a^{-1}. The entire watershed is dominated by tiny erosion, but the intensity of erosion gradually increases from the centre to the periphery. The erosion at the south and north ends of the watershed is most significant. A significant positive correlation was found among soil erosion, altitude and slope. As the altitude increases, the erosion becomes more intenser. As slope increases, the erosion becomes more significant. The average elevation increased by 200 m, and the degree of soil erosion increased by 1.24 times. For each level of slope increase, the soil erosion modulus increased by 497.28 t km^{-2} a^{-1}. Soil erosion mainly occurs in an area representing 17.73% of the basin. Additionally, soil erosion is mainly distributed among areas greater than 2,200 m above sea level and above 35°; thus, this region is the critical area of erosion limitation.

Keywords: GIS; RUSLE; Dianchi Lake basin; Soil erosion; Spatial distribution characteristics

1. Introduction

Soil erosion causes the loss of land resources and the decline in land productivity. In addition, because a large amount of sediment is washed into rivers and lakes, these water bodies experience increased sediment deposition, which reduces their flood storage capacity. This condition further leads to the natural disasters, such as droughts, landslides, floods and mudslides, and this reduced capacity seriously affects the comprehensive development and effective utilization of water and soil resources in a region, leading to soil degradation. At the same time, the nitrogen and phosphorus elements that are carried in the sediment increase the level of pollution in the receiving water bodies (e.g., lakes, rivers), threatening ecological balance, is endangering human health, the sustainable development being restricting economy and society, it has let human beings be caught in difficult position.

Grasping the geographical distribution of regional soil erosion is the key to regional soil erosion control, and this understanding is the key to determining and implementing effective erosion conservation measures. Since the variables of soil erosion are complex and difficult to determine accurately, identifying the geographical distribution of erosion risk areas has been challenging. It was after the integration of GIS technology and soil erosion models that this problem was gradually solved. Researchers from all over the world have conducted considerable research on this aspect, and

the results demonstrate that the integration of GIS technology and soil erosion models can not only identify the location of erosion but also analyse the geographical distribution pattern of soil erosion [1–4]. Because the revised universal soil loss equation (RUSLE) model is simple in form, requires easy-to-obtain data, is comprehensive in terms of factor consideration, and is clear in physical meaning, it has been widely adopted worldwide [5–8]. The integration of RUSLE and GIS has become a popular approach to the study of the geographical space distribution and spatial quantification of erosion. The existing research mainly focuses on determining the space distribution of regional erosion [2,9–11], assessing erosion risk areas [3,4,12–16], and assessing the evolutionary trend of the spatiotemporal patterns of soil erosion areas [17–20]. Ding et al. [21] analysed the fractal of the spatial pattern of soil erosion in Dianchi watershed. Zhao et al. [22] used GIS technology to assess the soil erosion risk grade and distribution on the Baoxiang River basin of Dianchi Lake. Other researchers have analysed the spatiotemporal evolution of erosion in the basin over the past 30 y using GIS and USLE [23–25].

However, research on the geographical distribution of erosion under the different topographic factors in this region has received little attention, but the topographical features related to the spatial distribution of erosion can provide decision-making support for erosion prevention and provide reference for the ecological protection of a river basin. So, it is necessary to research soil erosion status and geographical distribution features of the watershed. This paper, the integration of GIS technology with the RUSLE model attempts to illustrate the following two problems: (1) soil erosion status and spatial distribution characteristics of Dianchi watershed, China; (2) the change law of soil erosion under the influence of different topographic factors.

2. Study area and data

The Dianchi watershed lies in the central and Eastern Yunnan, southwest of Kunming City (Fig. 1). The basin has an area of 2,920 km^2. Dianchi lake seats in the middle of the watershed, having an area of 310 km^2. It is the largest plateau freshwater lake in Yunnan Province.

2.1. Geology and soil

The Dianchi watershed is seated in the tectonic basin at the southern end of the north-south tectonic belt of China. The geological structure is complex, the lake features a wide range of landforms, and the foundation is weak. The north-south structure is the main control structure in the area, and it is localized mainly in the southern and central parts of the watershed. The east-west structure is secondary, located primarily in a small area in the central and northern parts of the basin. The development of folds—mostly strip-like—in the basin is more prevalent, and a small part is broken into faults.

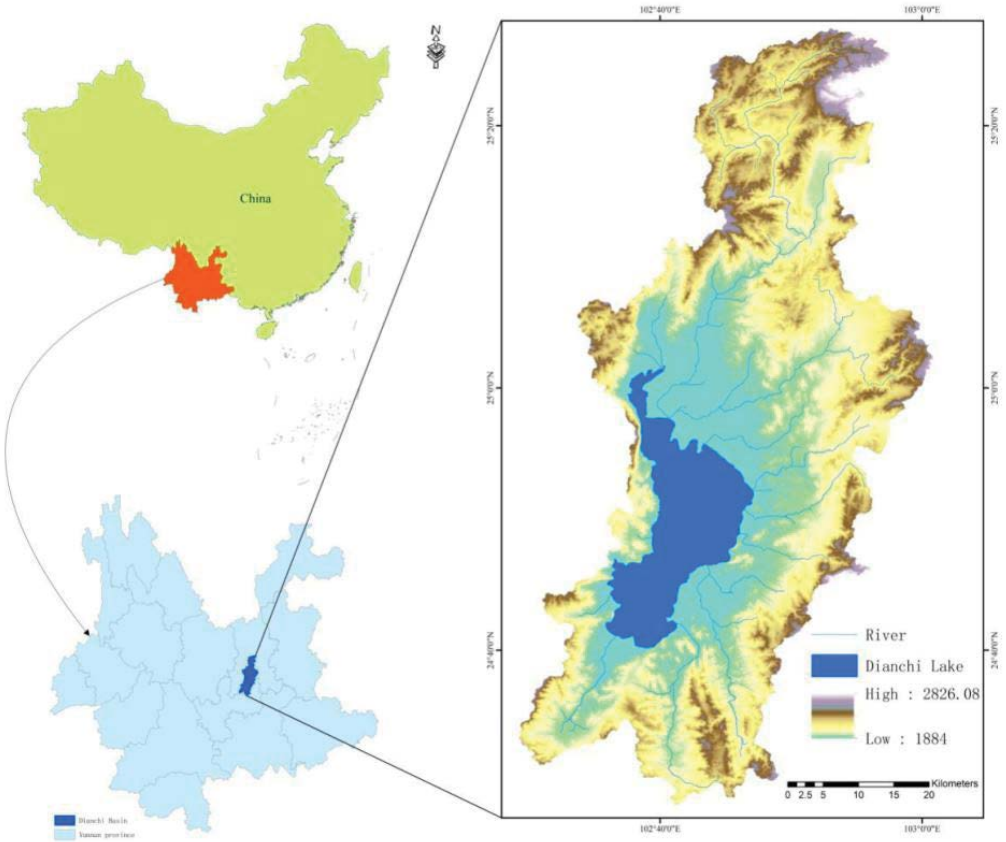

Fig. 1. Location map of Dianchi watershed.

The Dianchi Lake basin belongs to the plateau red soil area. According to soil survey data, the soil is dominated by red loam, purple soil and paddy soil. The vertical distribution of soil is not obvious, but due to differences in topography, soil quality and human utilization, the horizontal zonal distribution of soil is formed. Red soil is the dominant soil resource and is mainly distributed in mountainous areas and semi-mountainous areas with an altitude of 1,700–2,400 m. Purple soil and red soil are interlaced at gentle slopes and dam edges at an altitude of 1,800–2,200 m. Paddy soil is mainly distributed along rivers, dams and semi-mountainous areas. The pH value of the soil in the basin ranges between 4.0 and 7.5, the soil organic matter content is between 1.5% and 5.0%, the soil fertility is moderate, and the soil structure is good.

2.2. Geomorphology

Dianchi Lake is at the centre of the entire basin. The second largest dam in Yunnan Province—Kunming Dam—is close to the east, south and north of Dianchi Lake. The area of the dam is 764 km^2, and this area has the lowest elevation, the smallest slope and the flattest area in the basin. The dam is surrounded by mountains and hills. The height difference in the basin is nearly 1,000 m. The highest point is 2,826 m, and the lowest point is 1,884 m.

2.3. Meteorology

The Dianchi Lake basin sits down on the plateau, which has lower latitude. The geomorphology is diverse, and the terrain height difference is large. There are noticeable vertical differences and horizontal differences in terms of climate. According to the statistics of meteorological materials since 1949, the average annual temperature of the basin is 14.5°C. July is the hottest month in the basin, with an average temperature of 19.7°C. January is the coldest month with an average temperature of 7.5°C. Annual precipitation of about 924 mm, absolute humidity of 74%, humidity is not big, the annual frost-free annual average of more than 240 d.

2.4. Hydrology

Dianchi Lake belongs to a lake with faults, and the lake is similar to a bow in that it developed in the north-south direction. The longest span of the north-south direction is 40 km, the widest span of the east-west direction is 12.5 km, the average lake width is 7 km, the lakeshore line is 163.2 km long, and the area is approximately 306.3 km^2. There are greater than 20 perennial rivers that flow into Dianchi, and these rivers are arranged radially along the north, east and south of the lake. Among them, there are eight main inflow rivers, namely, Panlong River, Luolong River, Baoxiang River, Mayu River, Dongda River, Gucheng River, Layuhe River and Chaihe River. The water resources of the lake have been 900 million m^3 for many years. Tanglangchuan is the only exit channel in Dianchi Lake, and the outlet is located in Haimen Village, which is in the southwest corner of Dianchi Lake.

2.5. Data

The following data were used in this study, including: satellite images, soil, DEM, rainfall, etc. The details are shown in Table 1.

3. Model of soil erosion and parameter calculation

3.1. RUSLE model

The model of RUSLE can be traced back to the quantitative sedimentation studies of Abdullah et al. [26] and Miller [27] in Missouri in the United States in 1917. Since then, Cook [28] has proposed three core factors leading to erosion and sediment production: the type of soil texture, the erosion capacity of rainfall runoff, and vegetation's ability to protect soil.

Subsequently, Kamel et al. [29], and Wischmeier and Smith [30] constructed the Universal Soil Loss Equation (USLE) on the basis of rainfall runoff and sediment data from more than 10,000 plots at 49 sites over the past 30 y, which was obtained by the U.S. bureau of agricultural research. Under the leadership of relevant government departments in 1985, scientists further improved the USLE model based on new research results. In 1997, a revised version of the USLE model (RUSLE) is introduced [31]. The RUSLE model takes into account precipitation, soil erodibility, crop management, slope length and water and soil conservation measures. Because RUSLE has comprehensive considerations, the factors have physical meaning, simple forms, wide ranges of materials, and guarantees a certain precision; thus, this model has been widely used in the world. The expression of the model is as follows:

$$A = R \cdot K \cdot L \cdot S \cdot C \cdot P \quad (1)$$

where A is the annual average erosion modulus (t hm^{-2} a^{-1}); R is the rainfall erosivity factor (MJ mm hm^{-2} h^{-1} a^{-1});

Table 1
Data used in the study

No.	Data type	Source	Description
1	Rainfall data	Kunming Meteorological Bureau, China	Rainfall data for the year 2014 with five rain gauge stations
2	Soil data	Yunnan Province Soil Survey Office	Data of 16 soil types
3	Digital elevation model	http://www.gscloud.cn/	GDEMDEM 30 M (30-m resolution)
4	Satellite image	http://www.gscloud.cn/	Landsat 8 Image (year: 2014; resolution: 30 m)

K is the soil erodibility factor (t hm^2 h MJ^{-1} mm^{-1} hm^{-2}); L is the slope length factor; S is the slope steepness factor; C is the vegetation coverage and management factor; P is the soil and water conservation measure factor. Among them, L, S, C, and P are all dimensionless.

3.2. Rainfall erosivity factor (R)

Raindrops can splash and separate soil particles. Rainfall forms runoff and further washes and transports soil, creating erosion. Therefore, rainfall is a direct driver. Zhang and Fu [32] found through a large number of calculations that the error of rainfall erosivity obtained from daily precipitation is the smallest. Therefore, the rainfall erosivity model is constructed based on daily precipitation data. The model algorithm is shown in Eq. (2) as follows:

$$R_j = \sum_{i=1}^{k} \left(p_i\right)^{\beta} \tag{2}$$

where R_j is the rainfall erodibility of the j-th half month (MJ mm hm^{-2} h^{-1}). P_i is the daily rainfall of the i-th day in a half-month period (mm). K is the number of days in the half-month period. α and β are model parameters. In the model, if $P_i \le 12$ mm, the P_i value is counted as 0, while P_i is counted as the value. The α and β parameters reflect the rainfall characteristics of the area, and the calculation formula is as follows:

$$\beta = 0.8363 + \frac{18.144}{P_{d12}} + \frac{24.455}{P_{y12}} \tag{3}$$

$$\alpha = 21.586\beta^{-7.1891} \tag{4}$$

where P_{d12} is the average daily rainfall of 12 mm or more, and is the average annual rainfall of 12 mm or more. Using Eq. (2), the rainfall runoff erosivity of 2014 was calculated by the daily precipitation data of five monitoring points in Dianchi watershed, and the spatial pattern map of rainfall erosivity was generated by using the interpolation function of GIS (Fig. 2).

3.3. Soil erodibility factor (K)

K is an index to evaluate the vulnerability of soil to erosive forces, and it reflects the soil erodibility to the transportation and separation of erosivity. The value of K can be determined by many ways. There are many methods to determine K value, the most commonly used is the median particle size method, regression calculation method, EPIC model and so on. The calculation of many of the above methods requires a lot of soil property parameters, such as soil texture, structure, organic matter content permeability, etc., while the soil structure level permeability level is difficult to obtain. Among these methods, the EPIC model, which was improved by Wischmeier and Smith [30], is widely used because of the easy-to-obtain required factors such as sand, clay, powder and organic matter. The calculation model is given in Eq. (5) as follows:

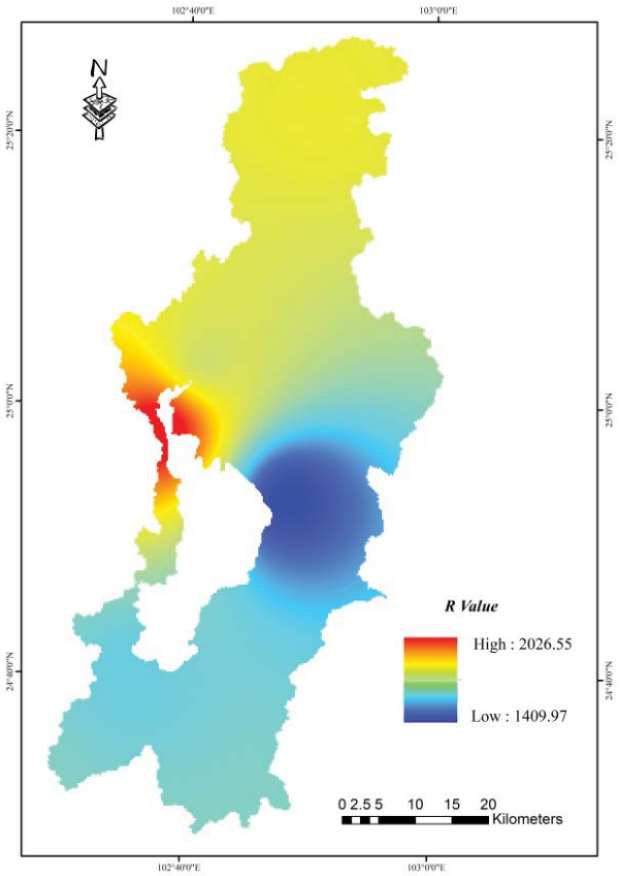

Fig. 2. Spatial pattern of R factor.

$$K_{\mathrm{EPIC}} = 0.1317\left\{0.2 + 0.3\exp\left[-0.0256\mathrm{SAD}\left(1 - \frac{\mathrm{SIL}}{100}\right)\right]\right\} \cdot \left[\frac{\mathrm{SIL}}{\mathrm{CLA} + \mathrm{SIL}}\right]^{0.3} \cdot \left\{1.0 - \frac{0.25C}{C + \exp\left(3.72 - 2.95C\right)}\right\} \cdot \left[\frac{\mathrm{SIL}}{\mathrm{CLA} + \mathrm{SIL}}\right]^{0.3} \cdot \left\{1.0 - \frac{0.25C}{C + \exp\left(3.72 - 2.95C\right)}\right\} \cdot \left\{1.0 - \frac{0.7\left(1 - \mathrm{SAD}/100\right)}{\left(1 - \mathrm{SAD}/100\right) + \exp\left(-5.51 + 22.9\left(1 - \mathrm{SAD}/100\right)\right)}\right\} \tag{5}$$

where SAD is the sand content (%), SIL is the powder content (%), CLA is the clay content (%), and C is the organic matter content (%). The organic matter content and mechanical composition of all kinds of soil types in the basin is obtained by querying "Yunnan Soil Species" (Yunnan Soil Census Office, 1992). By using GIS technology to spatially express the soil erodibility factor (K) in Dianchi Lake basin, spatial distribution of K is obtained (Fig. 3).

It can be seen from the K value diagram in Fig. 2 that the K value of most areas in the basin is between 0.15 and 0.18, and the area with the largest K value is at the northern end of the basin and a small part of the eastern region; moreover, the lowest K value is mostly distributed in the southern section of the basin.

3.4. Slope length and steepness factor (LS)

Slope length affects the flow velocity of the surface runoff. Generally, longer slope lengths generate faster surface runoff and greater erosive forces to the surface soil. In this paper, the calculation formula put forward by Wischmeier and Smith [30] was adopted to calculate the LS.

$$L = \left(\frac{l}{22.13}\right)^m \tag{6}$$

where L is the slope length factor, l is the slope length value, and m is the slope length index. m is calculated as follows.

$$m = \begin{cases} 0.5 & \beta \geq 2.86° \\ 0.4 & 1.72° \leq \beta < 2.86° \\ 0.3 & 0.57° \leq \beta < 1.72° \\ 0.2 & \beta < 0.57° \end{cases} \tag{7}$$

where β is the slope value.

Slope represents the degree of slope of the earth's surface, and its value directly affects the proportion and intensity of material flow and energy conversion, and is a direct factor affecting soil erosion. The slope calculation formula is shown in Eq. (8) as follows:

$$S = \left(65.41\sin^2\beta + 4.56\sin\beta + 0.065\right) \tag{8}$$

Eq. (9) can be obtained by integrating Eqs. (6)–(8).

$$\mathrm{LS} = \left(\frac{l}{22.13}\right)^m \times \left(65.41\sin^2\beta + 4.56\sin\beta + 0.065\right) \tag{9}$$

Based on DEM data of the watershed and the calculation formula for the slope length gradient factor, LS is calculated in the GIS environment, and the spatial pattern map of the LS is obtained (Fig. 4).

3.5. Cover and management factor (C)

In RUSLE model, C is the ratio of the amount of soil loss with field management or vegetation cover under certain conditions to the amount of soil loss on the bare ground under the same conditions, and this value is between 0 and 1. This value reflects the impact of vegetation cover and management on soil erosion. As the C value increases, the amount of soil erosion caused by this type of land use also increases. At present, the C value can be acquired

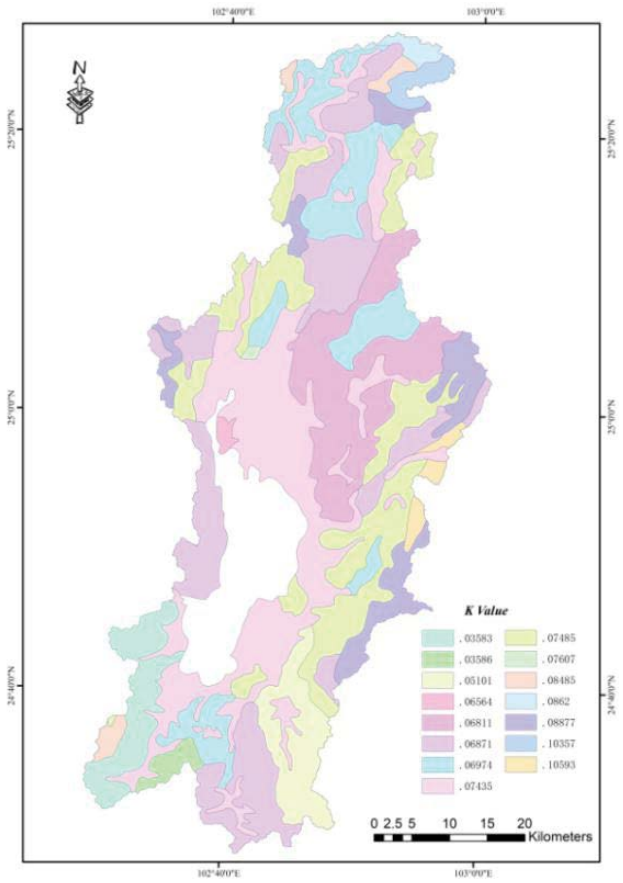

Fig. 3. Spatial pattern of K factor.

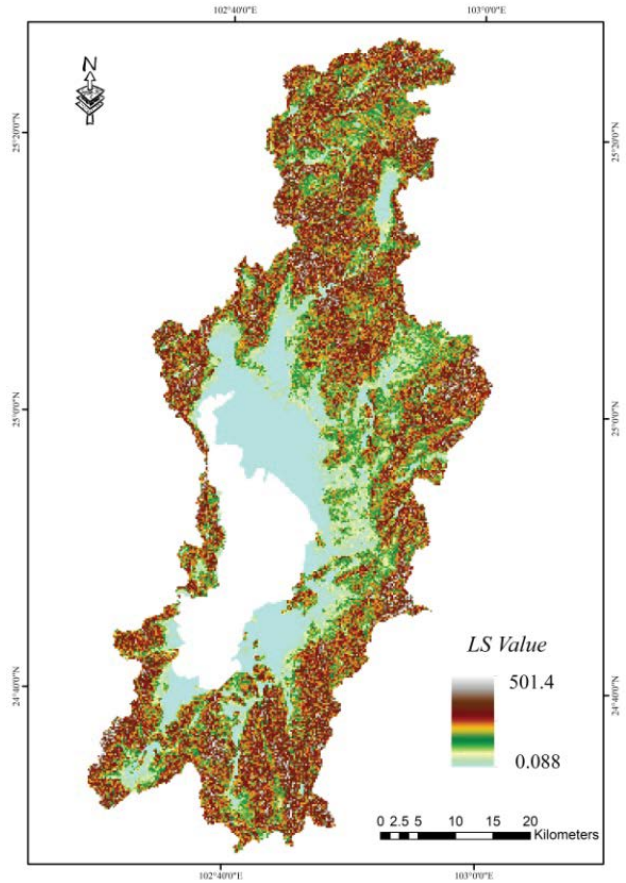

Fig. 4. Spatial pattern of LS factor.

by empirical methods and vegetation coverage calculation methods. The empirical method is mainly obtained through a large amount of statistical data, and the vegetation coverage is obtained by establishing a regression relationship equation. The *C* value calculation in this paper uses the *C* value model established by Cai et al. [35].

$$\begin{cases} C = 1 & c < 0 \\ C = 0.650\,8 - 0.343\,6\log c & 0 < c < 78.3\% \\ C = 0 & c > 78.3\% \end{cases} \quad (10)$$

where *c* is the vegetation coverage. After using the remote sensing image to get the vegetation coverage, spatial distribution of the *C* is obtained based on the above formula using ArcGIS software (Fig. 5).

3.6. Conservation practice factor (P)

P is a mixed model based on experimental and physical processes. The value ranges from 0 to 1. When the value of *P* is 0, it means the area where soil erosion will not happen at all, and when the value of *P* is 1, it means the area where no soil and water conservation measures have been taken. In large-scale soil erosion studies, field surveys and empirical methods are often used for comprehensive confirmation. The value of *P* in this paper is determined by referring to the previous studies and combining with the land use situation and soil and water conservation measures in the basin [22]. The results are shown in Table 2. The spatial pattern of the *P* is calculated based on the above formula using ArcGIS software (Fig. 6).

4. Results

4.1. Spatial pattern of soil erosion

Soil erosion amount of Dianchi watershed can be obtained by overlaying the five factors based on Eq. (1) using ArcGIS10.2. The soil erosion classification map of Dianchi

Table 2
The value of *P* in Dianchi watershed

Land use/land cover	*p*-value
Water body	0
Agriculture	0.59
Forest	1.0
Unused land	1.0
Built-up	0
Grass	1.0

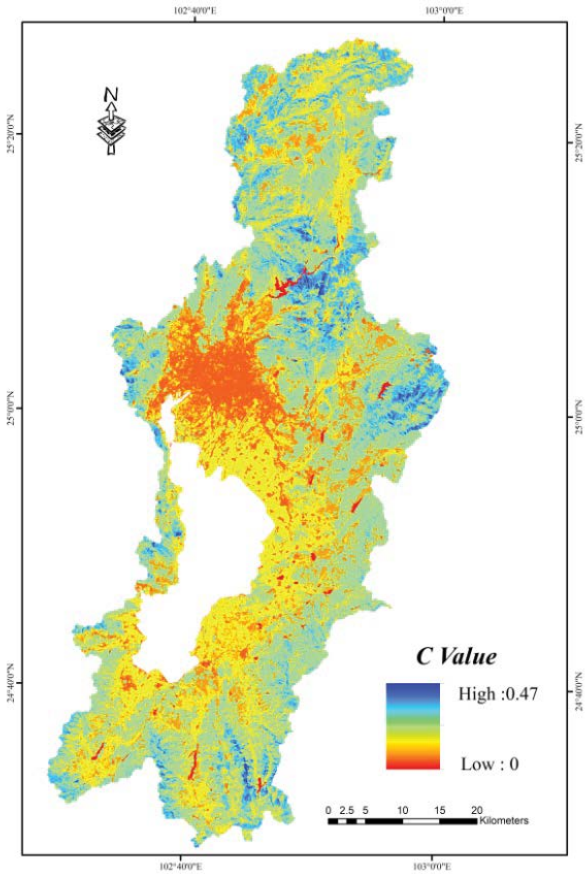

Fig. 5. Spatial pattern of *C* factor.

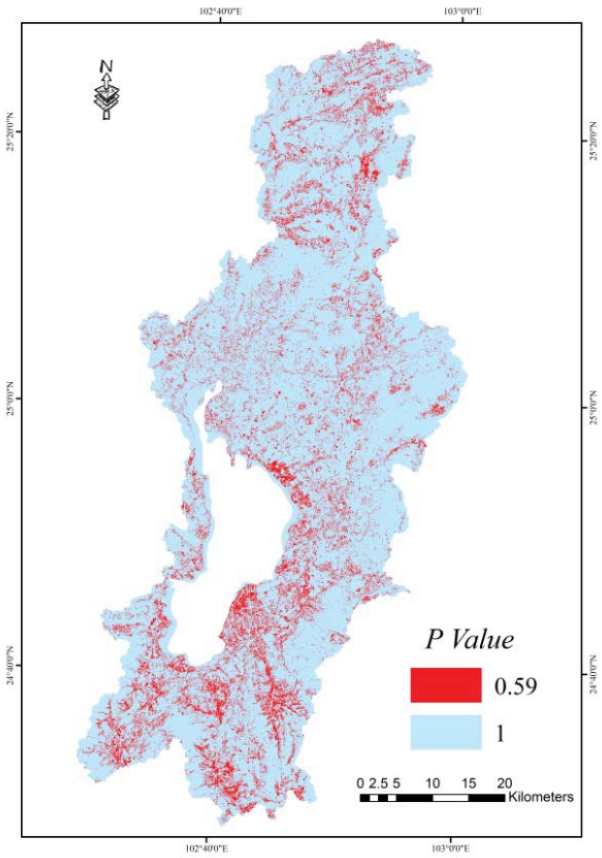

Fig. 6. Spatial pattern of *P* factor.

Lake basin can be obtained by classifying the results based on the Classification and Grading Standard of Soil Erosion (SL190-2007), which was formulated by the Ministry of Water Resources in 2007. The results (Fig. 7) show that the soil erosion in Dianchi Lake basin is mainly concentrated in the surrounding mountainous areas around Dianchi Lake and Kunming Dam, with the southern and northern ends of the basin having the most concentrated soil erosion.

By quantifying soil erosion amount in 2014, the results in Table 3 were obtained. The results show that the total erosion amount in the basin in 2014 was 2,250,100 t/a, and the average erosion modulus was 861.09 t km^{-2} a^{-1}, which represented moderate erosion. Based on the area occupied of erosion level, 82.29% of the area in the basin is tiny erosion. This indicates that most areas of the basin do not have erosion or erosion is not obvious. Other erosion areas have different degrees of erosion, accounting for 17.66% of the entire basin. Among them, moderate erosion areas only accounted for 8.72% of the area, and the total amount of erosion accounted for 41.71%, showing that erosion in Dianchi watershed is mainly characterized by moderate soil erosion in some areas. The severe erosion is small and positive, accounting for only 0.07% of the entire drainage area, which is almost negligible.

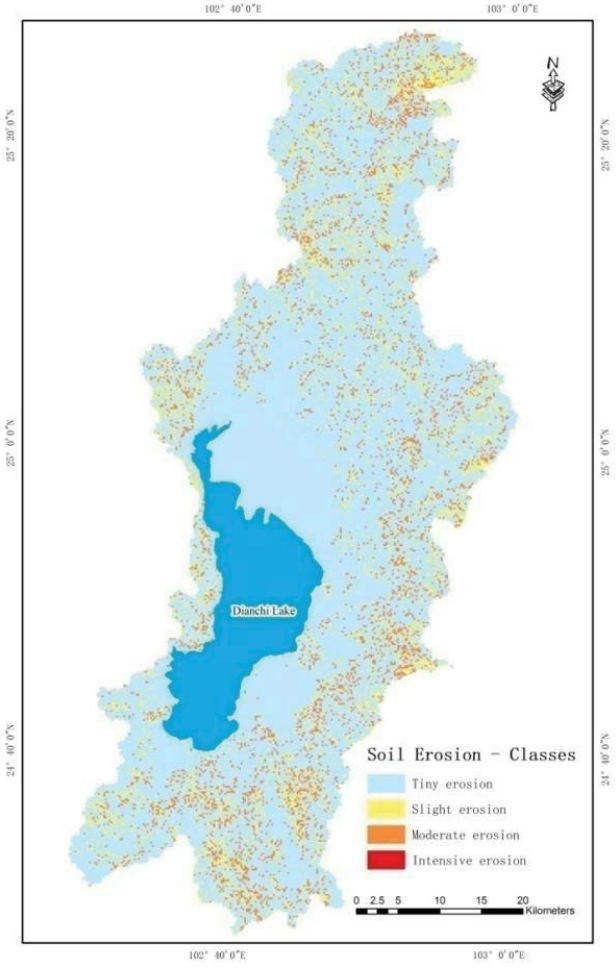

Fig. 7. Spatial pattern of classified soil erosion risk zones.

4.2. Altitude spatial pattern of soil erosion

According to the altitude distribution, the basin is divided into five grades, as shown in Table 4 and Fig. 8. It can be seen that soil erosion in the basin is closely related to altitude. With the increase in altitude, soil erosion rapidly increases. On average, the degree of soil erosion increases by 1.24 times for every 200 m increase. The growth rate of erosion is irregular, increasing from below 2,000 to 2,400 m, and the degree of erosion is doubled for every 200 m increase. An irregularity occurred from 2,200–2,400 m to 2,400–2,600 m, and the erosion increased more than three times. When the altitude increases from 2,400–2,600 m to more than 2,600 m, the growth rate of erosion is small. When the altitude is below 2,000 m, the average erosion modulus is 299.55 t km^{-2} a^{-1}, which represents tiny erosion. The average erosion modulus of 2,000–2,200 m and 2,200–2,400 m is 678.01 and 1,566.65 t km^{-2} a^{-1}, respectively, which represents slight erosion. The erosion increased sharply above 2,400 m, and the average erosion modulus exceeded 5,000 t km^{-2} a^{-1}, which represents moderate erosion.

4.3. Slope spatial pattern of soil erosion

Based on the SL190-2007 standard, the watershed slope is classified as six grades, and erosion status of each grade slope is counted. The results (Table 5) show that there is a close relationship between erosion density and slope. The greater the slope, the greater the amount of erosion and the more serious the erosion. The average soil erosion modulus increases by 497.28 t km^{-2} a^{-1} for each level of slope increase. The average soil erosion modulus of 0–5° and 5–8° is less than 500 t km^{-2} a^{-1}, which represents tiny erosion. The areas of 8–15° and 15–25° have slight erosion, and areas above 25° have moderate erosion. The area with a slope greater than 35° accounts for 73.29% of the entire basin area.

Table 3
Degree of each level of soil erosion Dianchi Basin

Soil erosion level	Erosion grading standard (t km^{-2} a^{-1})	Area (km^2)	Area percentage (%)	Average erosion modulus (t km^{-2} a^{-1})	Erosion amount (ten thousand t a^{-1})	Percentage of erosion amount (%)
Tiny erosion	<500	2,151.42	82.27	350.63	75.44	33.91
Slight	500~2,500	231.84	8.87	2,410.17	55.87	25.12
Moderate	2,500~5,000	228.03	8.72	4,069.1	92.79	41.71
Severe	5,000~8,000	1.76	0.07	5,157.32	0.91	0.41

Table 4
Amount of soil erosion at different elevation levels in Dianchi Basin

Altitude	Area (km^2)	Area percentage (%)	Average erosion modulus (t km^{-2} a^{-1})	Erosion amount (ten thousand t/a)	Percentage of erosion amount (%)
<2,000	1,055.92	40.41	299.55	31.63	14.06
2,000~2,200	967.4	37.02	678.01	65.59	29.15
2,200~2,400	494.43	18.92	1,566.65	77.46	34.43
2,400~2,600	69.69	2.67	5,015.07	34.95	15.53
>2,600	25.61	0.98	6,005.47	15.38	6.84

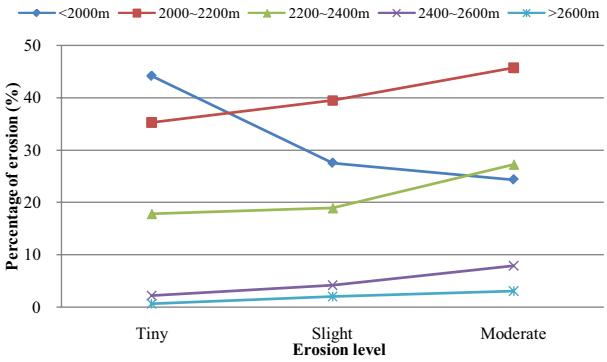

Fig. 8. Percentage of erosion at different soil degrees at different elevations.

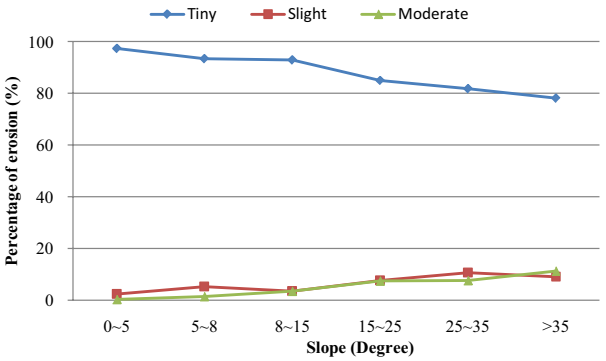

Fig. 9. Area percentages of different soil erosion degrees at different slope levels.

This area also experiences the most serious soil erosion. The amount of erosion accounts for 82.4% of the total erosion in the entire watershed, which means this region represents an important area for controlling soil erosion. From the perspective of the composition of different grades of erosion (Fig. 9), the distribution of different soil erosion grades on different slopes is quite different. Overall, the proportion of tiny erosion decreases as the slope increases. The area of tiny erosion is close to 100% on the slope of 0~5° and drops to 78.10% above 35°. Moderate erosion has the opposite trend, accounting for only 0.30% at 0~5° and rapidly increasing to 11.26% above 35°, which further reflects the relation between erosion and slope. This result shows that there is a significant positive correlation between soil erosion and slope. As the slope becomes steeper, the erosion becomes more obvious. When the slope is smaller, the degree of erosion is weaker.

5. Discussion

Based on GIS and RUSLE models, this paper studied the spatial pattern of soil erosion in Dianchi watershed in 2014. The results show that the entire basin is dominated by small amounts of erosion, and only 17.66% of the area has different degrees of erosion, including slight erosion and moderate erosion. The area of severe erosion is only 1.76 km^2, which is almost negligible. In terms of spatial distribution, soil erosion is mainly distributed around Dianchi Lake and Kunming Dam, and it is most concentrated at the southern and northern ends. Topographical factors such as altitude and slope have remarkable influence on soil erosion intensity. As the altitude and slope increase, soil erosion amount increases, the proportion of tiny erosion area gradually decreases, and the proportion of areas with other erosion intensities gradually increases. The erosion increased sharply above 2,400 m,

Table 5
Amount of soil erosion of different slope levels in Dianchi basin

Slope	Area (km^2)	Area percentage (%)	Average erosion modulus (t km^{-2} a^{-1})	Erosion amount (ten thousand t/a)	Percentage of erosion amount (%)
0~5	220.85	8.45	175.23	3.87	1.72
5~8	53.91	2.06	409.94	2.21	0.98
8~15	127.35	4.87	646.25	8.23	3.66
15~25	124.16	4.75	727.29	9.03	4.01
25~35	171.75	6.57	881.51	15.14	6.73
>35	1,915.03	73.29	974.03	186.53	82.90

and the average erosion modulus exceeded 5,000 t km^{-2} a^{-1}, which represented moderate erosion. The erosion is most serious at slopes above 35°, and this erosion accounts for 82.90% of the total erosion in the basin. Therefore, in view of the severely eroded areas described above, soil erosion should be controlled using biological measures, engineering measures and agricultural measures in accordance with the local conditions. In areas with complex topography and harsh conditions, prevention should be the main priority to reduce the threat to human life and property caused by geological disasters, such as mudslides and landslides.

References

[1] S. Alice, P. Christian, Erosion extension of indurated volcanic soils of Mexico by aerial photographs and remote sensing analysis, Geoderma, 117 (2003) 367–375.

[2] A. Pandey, V.M. Chowdary, B.C. Mal, Identification of critical erosion prone areas in the small agricultural watershed using USLE, GIS and remote sensing, Water Resour. Manage., 21 (2007) 729–746.

[3] V. Prasannakumar, H. Vijith, S. Abinod, N. Geetha, Estimation of soil erosion risk within a small mountainous sub-watershed in Kerala, India, using Revised Universal Soil Loss Equation (RUSLE) and geo-information technology, Geosci. Front., 3 (2012) 209–215.

[4] J. Thomas, S. Joseph, K.P. Thrivikramji, Assessment of soil erosion in a tropical mountain river basin of the southern Western Ghats, India using RUSLE and GIS, Geosci. Front., 9 (2018) 893–906.

[5] A.A. Millward, J.E. Mersey, Adapting the RUSLE to model soil erosion potential in a mountainous tropical watershed, Catena, 38 (1999) 109–129.

[6] M. Kouli, P. Soupios, F. Vallianatos, Soil erosion prediction using the revised universal soil loss equation (RUSLE) in a GIS framework, Chania, Northwestern Crete, Greece, Environ. Geol., 57 (2009) 483–497.

[7] H.R. Naqvi, J. Mallick, L.M. Devi, M.A. Siddiqui, Multi-temporal annual soil loss risk mapping employing revised universal soil loss equation (RUSLE) model in Nun Nadi watershed, Uttrakhand (India), Arab. J. Geosci., 6 (2013) 4045–4056.

[8] S. Galdino, E.E. Sano, R.G. Andrade, C.R. Grego, S.F. Nogueira, C. Bragantini, H.G. FlosiAna, Large-scale modeling of soil erosion with RUSLE for conservationist planning of degraded cultivated Brazilian pastures, Land Degrad. Dev., 27 (2016) 773–784.

[9] S. Beskow, C.R. Mello, L.D. Norton, N. Curi, M.R. Viola, J.C. Avanzi, Soil erosion prediction in the Grande River Basin, Brazil using distributed modeling, Catena, 79 (2009) 49–59.

[10] Y.H. Zhuang, C. Du, L. Zhang, Y. Du, S.S. Li. Research trends and hotspots in soil erosion from 1932 to 2013: a literature review, Scientometrics, 105 (2015) 743–758.

[11] L. Tamene, Z. Adimassu, J. Ellison, T. Yaekob, K. Woldearegay, K. Mekonnen, P. Thorne, Q. BaoLe, Mapping soil erosion hotspots and assessing the potential impacts of land management practices in the highlands of Ethiopia, Geomorphology, 292 (2017) 153–163.

[12] O. Fistikoglu, N.B. Harmancioglu, Integration of GIS with USLE in assessment of soil erosion, Water Resour. Manage., 16 (2002) 447–467.

[13] P.P. Dabral, N. Baithuri, A. Pandey, Soil erosion assessment in a hilly catchment of north eastern India using USLE, GIS and remote sensing, Water Resour. Manage., 22 (2008) 1783–1798.

[14] Y.Q. Xu, P. Jian, X.M. Shao, Assessment of soil erosion using RUSLE and GIS: a case study of the Maotiao River watershed, Guizhou Province, China, Environ. Earth Sci., 56 (2009) 1643–1652.

[15] Y. Farhan, S. Nawaiseh, Spatial assessment of soil erosion risk using RUSLE and GIS techniques, Environ. Earth Sci., 74 (2015) 4649–4669.

[16] B.P. Ganasri, H. Ramesh, Assessment of soil erosion by RUSLE model using remote sensing and GIS-a case study of Nethravathi Basin, Geosci. Front., 7 (2016) 953–961.

[17] Z.B. Xin, J.X. Xu, X.X. Yu, Temporal and spatial variability of sediment yield on the Loess Plateau in the past 50 years, Acta Ecol. Sinica, 29 (2009) 1129–1139.

[18] Z.H. Yao, Q.K. Yang, Y.L. Wu, R. Li, Spatial-temporal dynamic features in soil erosion of the Gushanchuan basin in the past three decades, Geomat. Inf. Sci. Wuhan Univ., 39 (2014) 974–980.

[19] D.H. Alexei's, D.G. Hadjimitsis, A. Athos, Integrated use of remote sensing, GIS and precipitation data for the assessment of soil erosion rate in the catchment area of "Yialias" in Cyprus, Atmos. Res., 131 (2013) 108–124.

[20] D.T. Meshesha, A. Tsunekawa, M. Tsubo, N. Haregeweyn, Dynamics and hotspots of soil erosion and management scenarios of the Central Rift Valley of Ethiopia, Int. J. Sediment Res., 27 (2012) 84–99.

[21] J.H. Ding, F.F. Xie, L. Chen, Fractal characteristics of spatial structure of soil erosion in Dianchi Basin, Soil Water Conserv. China, 1 (2011) 43–45.

[22] L. Zhao, G.L. Yuan, Y. Zhang, H.E. Bin, Z.H. Liu, Z.Y. Wang, J. Li, The amount of soil erosion in Baoxiang Watershed of Dianchi Lake based on GIS and USLE, Bull. Soil Water Conserv., 27 (2007) 42–46.

[23] L. Dong, M.C. Peng, C.Y. Wang, J.H. Du, Z.L. Chen, W.L. Kong, Research on soil erosion based on the USLE Model and RS/GIS in the Dianchi Lake watershed, Res. Soil Water Conserv., 19 (2012) 11–18.

[24] H.Y. Liu, C. Wang, Z.S. Lin, H. Yang, Dynamical monitoring of water loss and soil erosion in Dianchi Lake basin based on RS and GIS, J. Nanjing Norm. Univ., 35 (2012) 120–124.

[25] S.Y. Peng, K. Yang, L. Hong, Q.L. Xu, Y.J. Huang, Spatio-temporal evolution analysis of soil erosion based on USLE model in Dianchi Basin, Trans. Chin. Soc. Agric. Eng. (Transactions of the CSAE), 34 (2018) 138–146.

[26] N.S. Abdullah, M.A. Naim, N. Mohd-Nor, Z.A. Zainal Abidin, Diversity of cultivable bacteria by strategic enrichment isolated from farmed edible red seaweed, *Gracilaria* Sp., J. Clean WAS, 4 (2020) 17–20.

[27] M.F. Miller, Waste through soil erosion, Agron. J., 18 (1926) 153–160.

[28] H.L. Cook, The nature and controlling variables of the water erosion process, Soil Sci. Soc. Am. J., 1 (1937) 487–494.

[29] K. Kamel, S. Kaouther, B. Kaddour, Assessment of soil erosion by Rusle model in the mellegue watershed, Northeast of Algeria, Environ. Ecosyst. Sci., 4 (2020) 15–22.

[30] W.H. Wischmeier, D.H. Smith, Predicting Rainfall Erosion Losses - A Guide to Conservation Planning, Agriculture Handbook, 1978, p. 537.

[31] K.G. Renard, G.R. Foster, G.A. Weesies, D.K. Mccool, D.C. Yoder, Predicting soil erosion by water: a guide to conservation planning with the Revised Universal Soil Loss Equation (RUSLE), Agricultural Handbook, 1997.

[32] W.B. Zhang, J.S. Fu, Rainfall erosivity estimation under different rainfall amount, Resour. Sci., 25 (2003) 35–41.

[33] B. Prabal, H.R. Syed, B. Suman, M.M.R. Ismail, Climate change vulnerability and responses of fisherfolk communities in the South-Eastern Coast of Bangladesh, Water Conserv. Manage., 4 (2020) 20–31.

[34] Yunnan Soil Census Office, Yunnan Soil Species, Yunnan Science and Technology Press, Kunming, 1992.

[35] C.F. Cai, S.W. Ding, Z.H. Shi, Study of applying USLE and geographical information system IDRISI to predict soil erosion in small watershed, J. Soil Water Conserv., 14 (2000) 19–24.